DOI: 10.24996/ijs.2026.67.7.5

ISSN: 0067-2904

Removal of reactive blue RB238 azo dye by Ni-Cu nanoparticles produced using eucalyptus leaf extract

Hasan Fadhil Al Rubai*, Ghazi M.Abed, Basim A.Hussain
Scientific Research Commission, Research and Technology Center of Environment, Water and Renewable Energy, Baghdad, Iraq

Received: 26/11/2024 Accepted: 20/8/2025 Published: 30/ 7/2026

Abstract

This paper aims to develop an effective method for removing organic dye from polluted water by adsorption using nanoparticles prepared from eucalyptus leaf extract. Synthetic dyes, particularly azo dyes, have attracted significant attention due to their toxic and harmful impacts on human health and the environment. In this context, an eco-friendly green synthesis method utilizing eucalyptus leaf extract was employed to prepare nickel-copper nanoparticles (Ni-Cu NPs). The nanoparticles were characterized using X-ray diffraction (XRD), Fourier transform infrared spectroscopy (FTIR), atomic force microscopy (AFM), and scanning electron microscopy (SEM). AFM images showed that the nanoparticle sizes ranged from 10 to 40 nm in great abundance. These results are in agreement with the calculations made using the Debye-Scherrer equation, where the crystallite size of the three main peaks was found to be (32, 19, 21) nm. The removal of Reactive Blue 238 dye (RB238) using nanoparticles was investigated. The dye removal effectiveness was found to be dependent on the initial pH (3.5-9) and temperature (293-313K), as well as the concentration of Eucalyptus nickel and copper nanoparticles, or (E-Ni-Cu/NPs) (0.5-2.5 $g.L^{-1}$) and dye (25-100 $mg.L^{-1}$). With an appropriate adsorbent concentration of 0.1 g per 25 $mg.L^{-1}$ and an acidic medium with a pH of 3.5, it was found that 293K would produce the best decolourization of 100% in 45 minutes. The results of the kinetic adsorption models indicate a pseudo-second-order model.

Keywords: Adsorption, green synthesis, metal nanoparticles, reactive blue 238,removal.

ازالة صبغة الازو الزرقاء التفاعلية RB238 بوساطة دقائق نانوية من النحاس والنيكل انتجت باستخدام مستخلص اوراق الكالبتوز

حسن فاضل الربيعي * ، باسم عبد الستار حسين ، غازي محمد عبد
مركز بحوث وتكنولوجيا البيئة والمياه والطاقات المتجددة ، هيئة البحث العلمي ، بغداد ، عراق

الخلاصة

يهدف هذا البحث إلى تطوير طريقة فعالة لإزالة الصبغة العضوية من المياه الملوثة عن طريق الامتزاز باستخدام الجسيمات النانوية المحضرة من مستخلص أوراق الكالبتوز. اكتسبت الصبغات الصناعية اهتمامًا

*Email: hasanfalrubai66@gmail.com

Open Access Articles. This articles is licensed under CC BY

كبيرًا في الوقت الحاضر، وخاصة الصبغات الأزو الأكثر شيوعًا، نظرًا لتأثيراتها الضارة والسامة على صحة الإنسان والبيئة. تم استخدام عملية التوليف الأخضر الصديقة للبيئة لإعداد جسيمات نانوية من النيكل والنحاس. تم توصيف الجسيمات النانوية باستخدام حيود الأشعة السينية ،مطيافية الأشعة تحت الحمراء ، مجهر القوة الذرية، والمجهر الإلكتروني الماسح. وأظهرت صور المجهر الذري أن أحجام الجسيمات النانوية تتراوح من 10 إلى 40 نانومتر بوفرة كبيرة. تتفق هذه النتائج مع الحسابات التي أجريت باستخدام معادلة ديباي–شرير حيث وجد أن حجم البلورة للقمم الرئيسية الثلاثة هو (32، 19، 21) نانومتر.تم التحقق في إزالة الصبغة الزرقاء الفعالة 238باستخدام سطح الدقائق النانوية. وجدت النتائج أن كفاءة إزالة الصبغة تعتمد على تركيز الدقائق النانوية 0.5 – 2.5غم لكل لتر، وتركيز الصبغة 25–100 ملغم / لتر، والرقم الهيدروجيني الأولي 3.5 – 9 ودرجة الحرارة 293 – 313 درجة مطلقة . باستخدام تركيز مناسب للمادة المازة قدره 0.1 غرام لكل 50 ملغم/لتر، وسط حمضي بدرجة 3.5، و 293 كلفن يُنتج افضل إزالة لون بنسبة 100% في 45 دقيقة. تشير نتائج نماذج الامتزاز الحركي إلى أنموذج حركي من المرتبة الثانية الزائفة.

1. Introduction

Wastewater comprises waste materials from various industries, with the textile sector being a major contributor due to its extensive use of water and chemicals [1]. Reactive Blue 238, an azo dye, is widely used in the textile industry due to its features of full color, bright colors, high washing fat, various reactants, different temperatures, various application methods and inexpensive application [2]. The presence of color in textile industry effluents makes their wastewater particularly challenging to treat. Dyes in water give out a bad color and can cause diseases like haemorrhage, ulceration of the skin, nausea, severe irritation of the skin and dermatitis [3]. The world's sources of clean, uncontaminated water are seriously threatened when even trace amounts of trash from these companies are released into the environment [4]. Many biological, physical, and chemical treatments can be used to remove pollutants, but these techniques are expensive and not environmentally friendly [5]. The development of green synthesis techniques in the latter half of the 20th century enabled the production of nanomaterials for their special properties, which paved the way for their use in a range of fields and industries, including industry, medicine, and chemistry [6]. One practical, affordable, and environmentally acceptable way to get rid of organic contaminants is by using adsorption technology on the surfaces of bimetallic nanoparticles, especially colors utilized in the textile sector [7]. Eucalyptus is the name of a genus of trees in the Myrtaceae family [8]. It is native to Australia and is part of a large genus that has over 600 species that can reach heights of 60 meters or more [9]. The limonene, cineole, betaine, and other antioxidants included in eucalyptus leaves work to reduce the valence of positive salt ions to zero [10, 11]. Metal nanoparticles Ag, Au, Pt, and Pd belong to the periodic table's d-block elements. Because of these remarkable properties, these nanoparticles are considered noble, and they are also reasonably priced [12]. In contrast, the metal nanoparticles Cu, Ni, Co, Fe, and Mo are less costly and share similar properties with noble nanoparticles [13, 14]. This study aimed to investigate the use of laboratory-synthesized E-Ni-Cu/NPs to remove the color of RB 238 from industrially polluted water, and to verify the suitability of this process for treating the azo dye. The kinetics of dye decolourization were studied using different concentrations of dye solution. The effects of E-Ni-Cu/NPs dosage, initial dye concentration, and solution pH on dye degradation were also investigated. Therefore, for the current study, an environmentally friendly synthesis method for E-Ni-Cu / NPs was used. The best conditions for obtaining the best dye removal will be researched through full batch experiments.

2. Experimental and Method

Chemicals and Reagents

Leaves of eucalyptus were collected from Baghdad Gardens. NaOH 1.0 M and H2SO4 1.0 M solutions, obtained from Appli Chem (GmbH), were used for pH adjustment. $CuSO_4.5H_2O$ was obtained from Fluka, while Ni $(NO_3)_2.6H_2O$ was supplied from BDH. RB238 was obtained from Ciba Specialty Chemicals and used without further purification. Table 1 shows the properties of this dye.

Table 1: Characteristics of RB238

Properties of RB238	
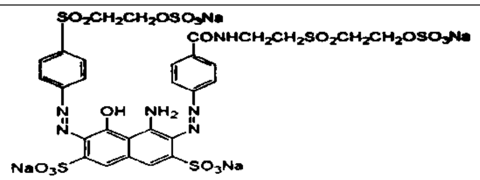	
C.I number	205055
Molecular formula	$C_{29}H_{26}N_6Na_4O_{20}S_6$
Molar mass	1062 g.mol^{-1}
Solubility in water	Water-soluble nature
λ max (nm)	605

Synthesis of the Adsorbent

Ni-Cu nanoparticles were synthesized using a modified version of a prior method [15]. First, the eucalyptus leaves were thoroughly washed and then soaked in hot distilled water for an hour at 353K, using a ratio of 100 grams of leaves for every litre of H_2O. Next, 250 mL of a 0.01 M mixed salt solution containing $Ni(NO_3)_2.6H_2O$ and $CuSO_4.5H_2O$ was prepared in a 500 mL beaker. The solution concentration was 0.01 M. Third, 100 mL of eucalyptus leaf extract was gradually added to the salt mixture while stirring constantly. A color change from a light blue to a greenish-black indicated the formation of zero-valent particles, which began to appear after an hour. Fourth, the nanoparticles were dried, stored, and periodically cleaned with distilled water before being used in the tests of this study.

Nanoparticle characterization techniques

A variety of analytical techniques were employed to characterize the generated nanoparticles. The mean diameter, shape, and topography of the E-Ni-Cu / NPs were analyzed using an SEM instrument (Vega III Czech Republic). An AFM can be used to identify the types of atoms present in a material and determine their locations on a three-dimensional surface map. XRD technology not only analyzes the crystallization of the nanomaterial but also aids in determining the crystallite size of the most common nanoparticles. Finally, accurate spectroscopic information regarding the general composition of the NPs was obtained using FT-IR spectroscopy.

Batch Experiments

In this study, the 100 mL dye solution used in this investigation was treated with nanoparticles (NPs) at concentrations ranging from 0.5 to 2.5 g.L^{-1}. The mixture was then immediately agitated using a thermostatically controlled shaker. The initial range of values for RB238 was 25–100 mg.L^{-1}, the temperature ranged from 293 to 313K, the pH ranged from 3.5 to 9, and the vibrator speed was 180 rpm. 5 ml of samples were taken out of the reaction vessel and centrifuged at predefined intervals (5, 10, 15, 25, 35, 45, and 60 minutes). The samples were then filtered through a 0.45 µm membrane filter. A Japanese-made (UV-Vis) device was used to measure the residual concentrations of the dyes under study at wavelengths of 605 nm.

Adsorption and the removal of this work used the following adsorption and removal equation
The following relationship was used to study the dye decolorization efficiency Eq.1

$$\text{Decolorization efficiency } \% = [(C_0 - C_t) / C_0] \times 100\ \% \quad (1)$$

Where the dye concentration at reaction time t, min; is denoted by C_t (mg.L^{-1}); and the starting dye concentration is represented by C_0 (mg.L^{-1}); Eq. 2 can be used to estimate the adsorption capacity at equilibrium q_e, which is defined as the ratio between the adsorbate quantities (mg) per adsorbent (g).

$$q_e = (C_0 - C_t)\, V / W \quad (2)$$

where V(L) ; is the volume of the solution being studied in liters and W(g) ; is the mass of the adsorbent.

3. Results and Discussion

Characterization of Nanoparticles

Using the XRD technique, the crystalline structure of E-Ni-Cu/NPs is shown in Fig. 1. The 2Θ values range from 20º to 80º. A prominent peak with an intensity of 287 is observed at 43.4°, which corresponds to copper [16]. It was noticed that cubic nickel particles correlate to a peak at 50.5º (69) [17]. However, the peak at 36º (95) appears, indicating the influence of nickel and copper in the crystal lattice [15]. The principal peaks were subjected to the Debye-Scherrer equation, Eq. 3, to estimate the crystalline size D of the (NPs).

$$D = K\lambda / \beta \cos \Theta \quad (3)$$

Where λ is the X-ray wavelength, equal to 1.5418 A^0, and K is the constant shape factor, equal to 0.9.β indicates the full-width half maximum (FWHM), and Θ represents the Bragg's angle. It was found the crystallite size of the three main peaks is (32, 19, 21) nm.

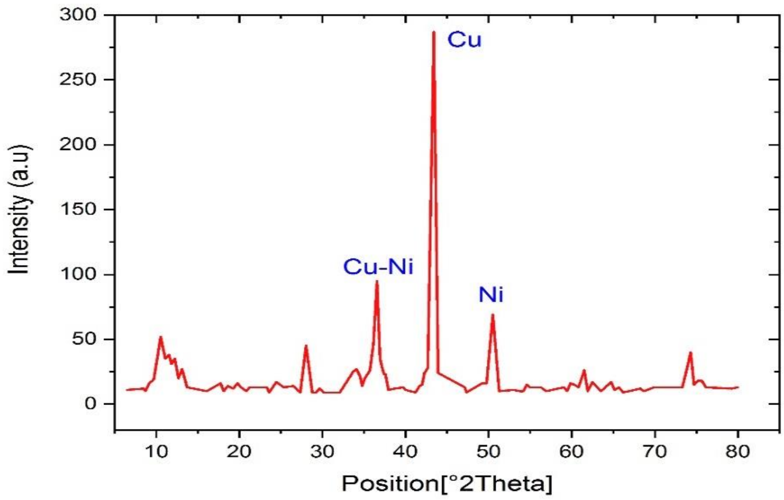

Figure 1: XRD of E-Ni-Cu/NPs

The nanoparticle morphology is depicted in Fig.1. SEM pictures, demonstrate their heterogeneous combination and the fact that their aggregation causes the particles to vary in size. The reasoning is that the size of the nanoparticles increases with the number of metal ions, or it might be because of their interaction with the extract [18], in which case the XRD pattern shows low levels of nickel content. The AFM images in Fig. 3 reveal the surface at a fine scale, below the atomic diameters, showing a substantial abundance of nanoparticles ranging in size from 10 to 40 nm. These findings agree with computations made with the Debye-Scherrer equation.

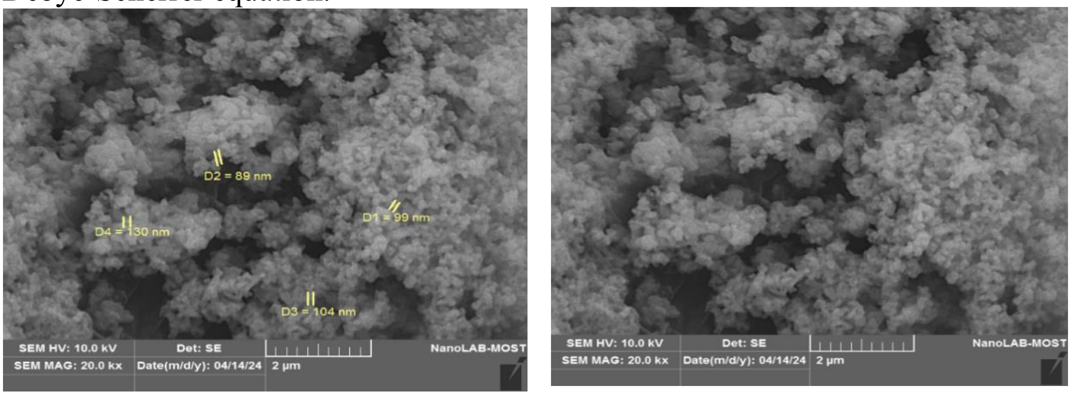

Figure 2. SEM images of E-Ni-Cu / NPs

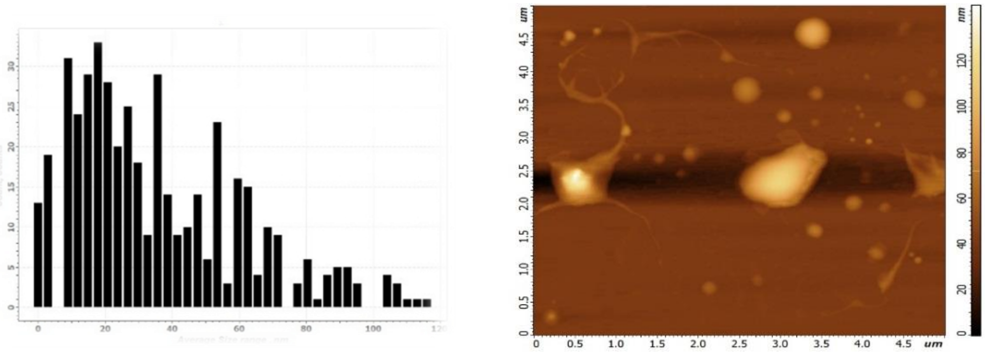

Figure 3: Photomicrograph of E-Ni-Cu / NPs using AFM.

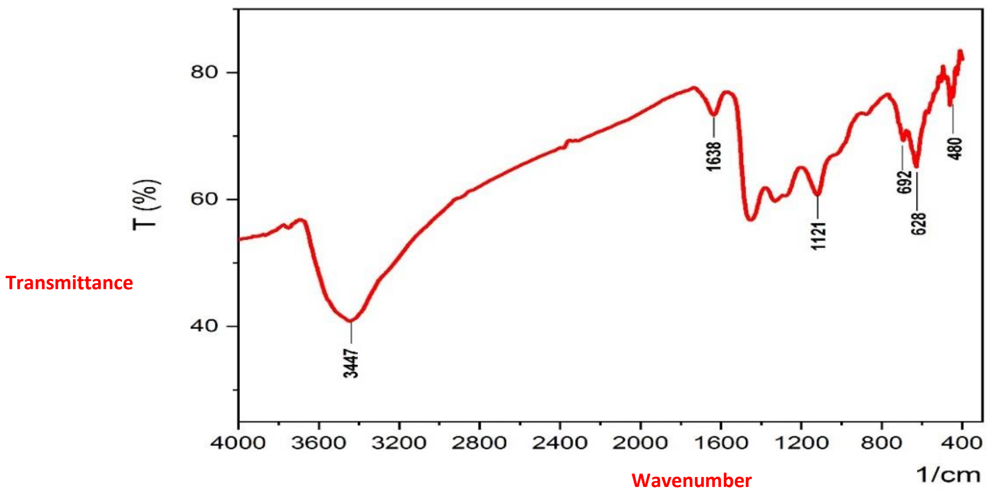

Figure 4: FTIR spectrum of E-Ni-Cu / NPs.

FTIR spectroscopy, which operates in the 400-4000 cm^{-1} range (Fig.4), shows four bands corresponding to water bending vibrations at 1637.5 cm^{-1}, and a broad peak related to water stretching vibration has a large peak at 3446.7 cm^{-1}. The FTIR peaks are impacted by the existence of organic compounds on the surface of nanoparticles [19]. A set of three peaks was observed at 480, 628, and 692 cm^{-1}, which may plausibly belong to carbon-metallic bonds, whereas there is a C-O absorption at 1120.6 cm^{-1} [20].

The effect of adsorbent dosage

The effects of altering the E-Ni-Cu / NPs dose on the dye RB238 elimination efficiency are shown in Fig. 5. It was demonstrated that this efficiency increases with increasing nanoparticle dose, and since the color removal efficiency at 95% was not significantly affected, employing dose greater than 0.1 g is not necessary. Consequently, this dosage was utilized in the following studies.

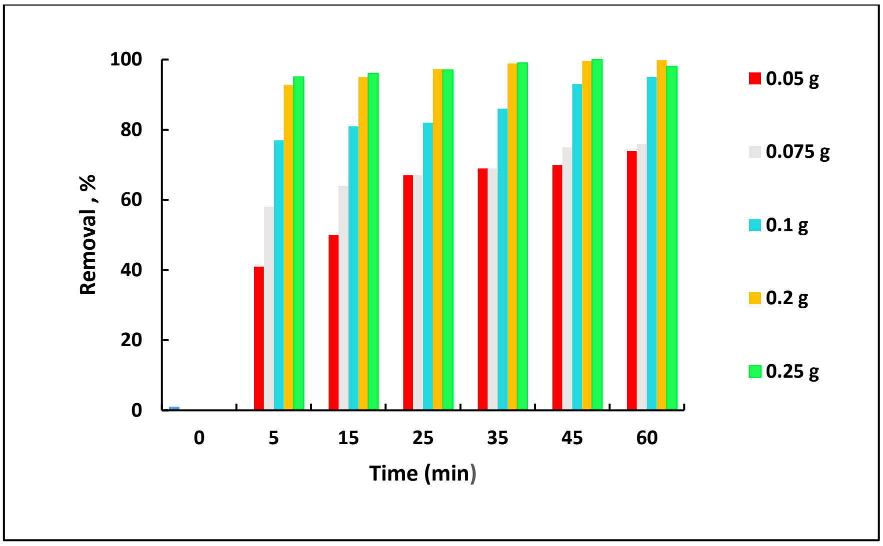

Figure 5: The impact of adsorbent dosage on decolorization efficiency at a temperature of 293 K, pH of 3.5, rpm of 180, contact period of 60 min, and dye concentration of 50 $mg.L^{-1}$.

Effect of the initial pH

The adsorption process is significantly influenced by the pH of the solution because variations in pH have an impact on the electrostatic interactions that take place at the adsorption surface as a result of the presence of ions in the reaction mixture. Figure 6 illustrates the degradation of RB238 dye under different acidic conditions, with pH values of 3.5, 7, and 9, respectively, after a contact time of 60 minutes. The degradation efficiency is 95, 57, and 58%. The reason for the decreasing removal effectiveness with increasing pH is most likely related to the effect of pH on the adsorbent's surface charge and degree of ionization [21].

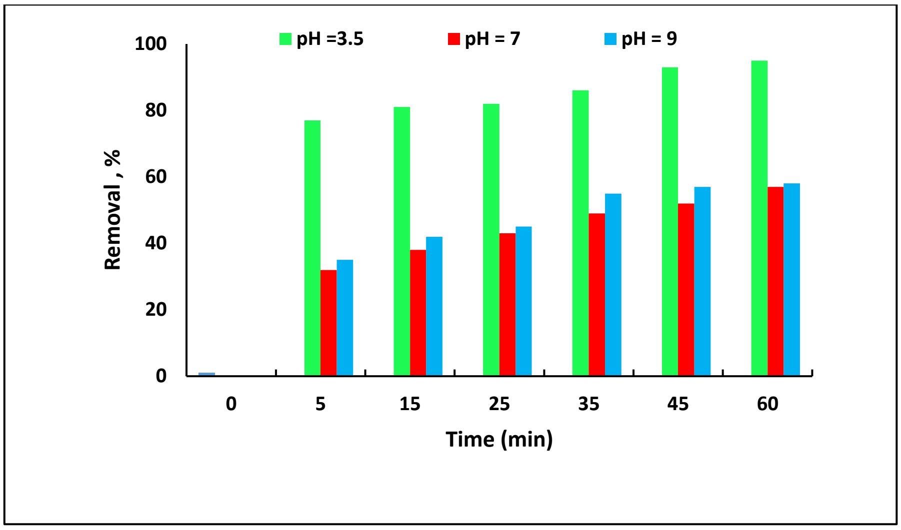

Figure 6: Effect of initial pH on decolorization efficiency (temperature = 293 K, adsorbent dosage = 0.1g, rpm = 180, and dyes concentration = 50 mg.L^{-1}).

Effect of initial dye concentration

The initial concentration of the dye solution is a crucial component that must be taken into account in order to achieve optimal adsorption because there is a transition between the dye's ionic and solid phases, as well as resistance during this change [22]. Figure 7 demonstrates the good color removal performance of the dye solution containing a modest concentration of RB238 (25 mg.L^{-1}). The dye solution achieved 90% at 35 minutes of contact time and 70% at 100 mg.L^{-1} concentration at the same contact period.

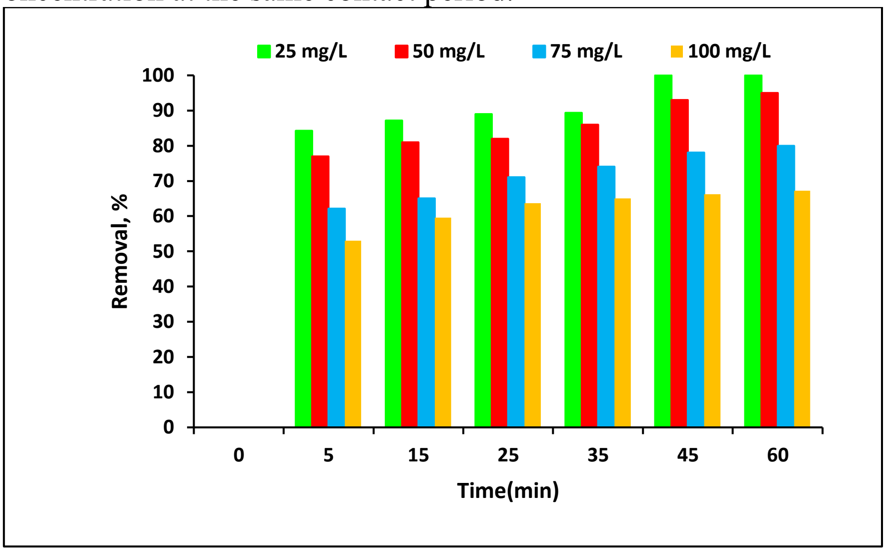

Figure 7: A comparison of the decolourization efficiency with different beginning dye concentrations at(temperatures 293 K, pH = 3.5, adsorbent dosage of 0.1g and rpm = 180)

The adsorbed dissolved on the surface of the nanoparticles compete with the active sites exposed to adsorption for the given number of sites, causing the reaction speed to slow down as the concentration of competing dye molecules increases [23].

Effect of temperature

The temperature factor is one of the key variables that influences how well dye degradation proceeds [24]. The impact of temperature variation on dye RB238 adsorption is depicted in Figure 8. When the temperature was raised from 293K to 303K and then 313K, the percentage of dye removal dropped from 95%, 92%, and 84% at a contact time of 60 minutes, respectively, indicating that the temperature change had no discernible effect on the dye's ability to adsorb on the surface of the nanoparticles. Dye adsorption is considered an exothermic process by nature, even though the decrease in dye degradation with increasing temperature is not significant [25].

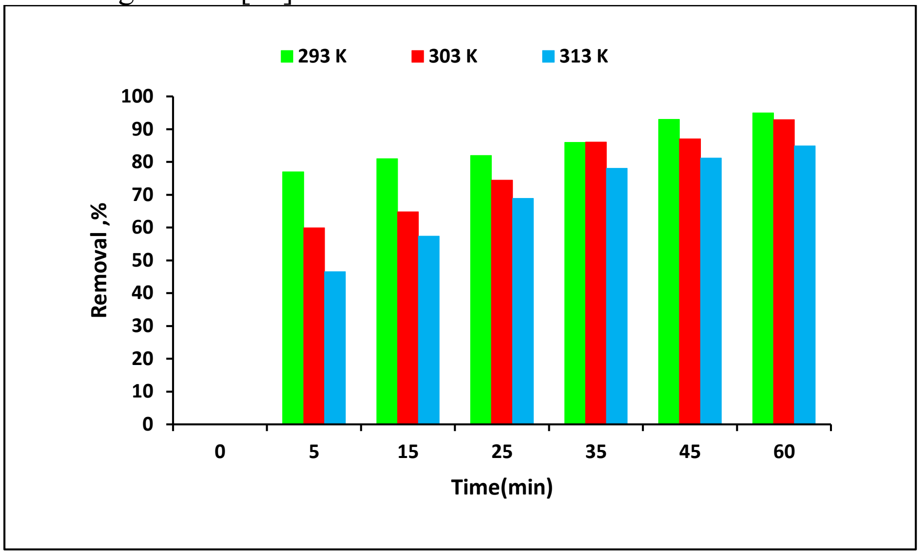

Figure 8 : Impact of temperature changes on decolorization efficiency (pH = 3.5, RB238 concentration = 50 mg .L^{-1}, adsorbent dosage = 0.1g, and rpm = 180)

Table 2: Kinetic models equation

Model	Equation	Parameters
Pseudo-first order	$\log(q_e - q_t) = \log q_e - \frac{k_1}{2.303} t$	q_t: adsorption capacities at time t (mg.g^{-1}) k_1: rate constant of pseudo-first order (min^{-1})
Pseudo –second order	$\frac{t}{q_t} = \frac{1}{k_2 q_e^2} + \frac{t}{q_e}$	k_2 : rate constant pseudo-second order (g/mg.min)
Elovich	$q_t = \frac{1}{\beta} \ln(\alpha \beta) + \frac{1}{\beta} \ln(t)$	α: initial rate constant of adsorption. (mg/g.min) β :desorption rate constant (g.mg^{-1})

Kinetic analysis of dye RB238 adsorption

Table 2 provides a summary of the formulas used to investigate the kinetics of dye RB238 adsorption. Pseudo-first, second and Elovich are the three kinetic models. For the adsorption kinetics to be consistent with the models previously mentioned, the retained model must be efficient, realistic, and have the highest coefficient R^2 [26]. Table 3 presents the adsorption constants from the experimental results, used to validate the suitability of the adsorption kinetic models, which serve as the key criteria for selecting the kinetic model. Plotting log (q_e –q_t) versus t yields a slope, as shown in Figure 9a, which represents the value of the constant k_1 for the pseudo-first-order model. On the other hand, the values of the constants k_2 and q_e can be determined from the slope of the pseudo-second-order model's graph when (t / q_t) vs t is plotted (Figure 9b). In Figure 9c, the slope of the variable q_t versus the ln t graph is used to calculate the constants β and α using the Elovich kinetic model. The values of α and β were found to be correlated with the initial dye concentration. Moreover, the low R^2 value of the Elovich model implies that it is not a suitable fit for kinetic application [27]. The regression coefficient R^2 of the pseudo-second-order model, which is higher than that of the pseudo-first-order model and its value for the Elovich model (Table. 3), indicates the most suitable kinetic model.

Table 3: The kinetic parameters for the adsorption of RB238 onto E-Ni-Cu / NPs at various initial dye concentrations and temperature=293K

RB238 ($mg.L^{-1}$)	$q_{e.exp}$ (mg/L)	Pseudo – first order k_1	Pseudo – first order R^2	Pseudo – second order k_2	Pseudo – second order R^2	Elovich – Model α	Elovich – Model β	Elovich – Model R^2
25	24.68	0.077	0.8206	0.038	0.9969	10.5	0.146	0.9026
50	45.34	0.085	0.7144	0.044	0.9985	27.11	0.083	0.7925
75	53.76	0.084	0.9139	0.019	0.9964	28.92	0.065	0.8592
100	69.81	0.089	0.8807	0.022	0.9988	37.31	0.054	0.8365

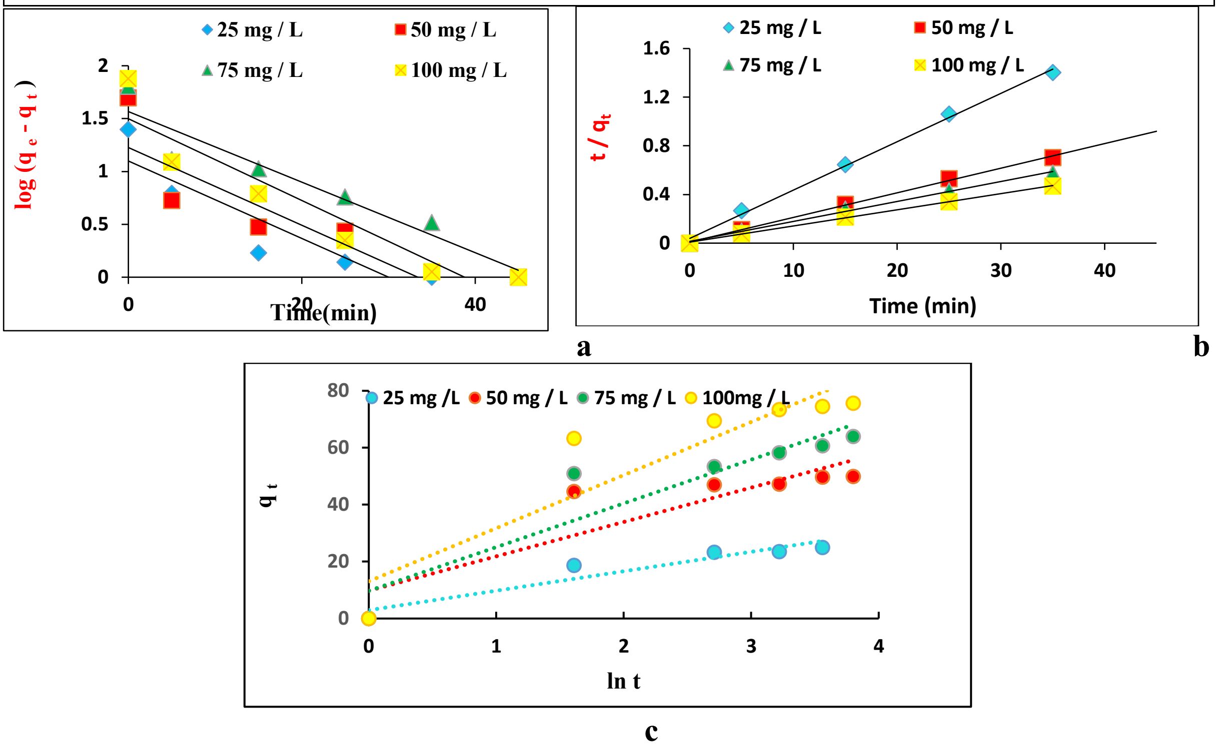

Figure 9: Kinetic models at a different initial concentration of RB238 adsorption.

Conclusion

This study focuses on enhancing the efficiency of metallic nanoparticles for organic dye removal while elucidating the underlying adsorption mechanisms. Employing eucalyptus leaf extract to prepare nanoparticles represents a greener approach compared to traditional chemical methods. Additionally, the combined use of copper and nickel nanoparticles (dual synthesis) demonstrates a superior dye removal effect compared to the use of either metal alone. Combining nanotechnology with green synthesis represents an environmentally sustainable solution for treating industrial pollution. This technology can be widely applied in industrial wastewater treatment, soil removal, and even in the pharmaceutical industry. The application of this technology to various types of organic dyes and other pollutants should be studied, and comprehensive environmental studies should be conducted to evaluate the potential environmental impacts of nanoparticles. Collaboration between researchers in various fields (nanotechnology, environment, chemical engineering) should be strengthened to promote research and development in this field.

5. Acknowledgments

The authors would like to express their gratitude to the Research and Technology Center of Environment, Water and Renewable and for Industrial Applications Research Center

Technology, cooperation in providing the necessary materials to successfully complete this research.

References

[1] Y. Y. Muhi-Alden and K. A. Salah, "Removing of methylene blue dye from its aqueous solution using polyacrylonitrile/iron oxide/graphene oxide," *Iraqi Journal of Science*, vol. 63, no. 6, pp. 2320–2330, 2022.

[2] D. R. Waring and C. Hallas, *The Chemistry and Application of Dyes*. Springer Science and Business Media, 2013.

[3] M. A. Rafique, S. Kiran, A. Jamal, S. Abrar, F. Jalal, and N. Rahman, "Nickel nanoparticles synthesized from *Psidium guajava* peels mediated degradation of Orange E3 dye: A sustainable approach," *International Journal of Environmental Science and Technology*, vol. 20, pp. 2733–2744, 2023.

[4] S. Shams, S. Kiran, T. Gulzar, and M. Anjum, "Synthesis and characterization of Ca-alginate/CuO bionanocomposite for removal of Reactive Yellow 145 dye: A green approach towards sustainability," *Clean Technologies and Environmental Policy*, vol. 26, pp. 3253–3271, 2024.

[5] S. Saed and D. E. Al-Mammar, "Influence of acid activation of a mixture of Illite, Kaolinite, and Chlorite clays on the adsorption of Methyl violet 6B dye," *Iraqi Journal of Science*, vol. 62, no. 6, pp. 1761–1778, 2021.

[6] M. Balamurugan, S. Saravanan, and T. Soga, "Synthesis of iron oxide nanoparticles by using *Eucalyptus* plant extract," *Journal of Surface Science and Technology*, vol. 12, pp. 363–367, 2014.

[7] H. F. AlRubai, A. K. Hassan, M. S. Sultan, and W. M. Bood, "Kinetic of adsorption of reactive red 120 using bentonite modified by CTAB and study the effect of salts," *Nature Environment and Pollution Technology*, vol. 20, no. 1, pp. 281–289, 2021.

[8] R. Amorati, M. C. Foti, and L. Valgimigli, "Antioxidant activity of essential oils," *Journal of Agricultural and Food Chemistry*, vol. 61, pp. 10 835–10 847, 2013.

[9] J. Silva, W. Abebe, S. Sousa, F. Matos, and V. Duarte, "Analgesic and anti-inflammatory effects of essential oils of eucalyptus," *Journal of Ethnopharmacology*, vol. 89, pp. 237–283, 2003.

[10] L. B. Makhlouf and K. Madani, "Total phenolic content, antioxidant and bacterial activities of fruits of *Eucalyptus globulus* cultivated in Algeria," *Industrial Crops and Products*, vol. 41, no. 1, pp. 85–89, 2021.

[11] O. S. Ali and D. E. Al-Mammar, "Adsorption of the color pollutant onto NiO nanoparticles prepared by a new green method," *Iraqi Journal of Science*, vol. 65, no. 4, pp. 1824–1838, 2024.

[12] F. Lu and D. Astruc, "Nanocatalysts and other nanomaterials for water remediation from organic pollutants," *Coordination Chemistry Reviews*, vol. 408, p. 213180, 2020.

[13] G. Sharma, A. Kumar, S. Sharma, and G. T. Mola, "Novel development of nanoparticles to bimetallic nanoparticles and their composites: A review," *Journal of King Saud University - Science*, vol. 31, pp. 257–269, 2019.

[14] H. F. Al Rubai, M. S. Sultan, and G. M. Abed, "Enhancing the removal efficiency of azo dye using sodium borohydride in the presence of inorganic nanocatalysts," *Green Analytical Chemistry*, vol. 12, p. 100194, 2025.

[15] M. Nasrollahzadeh, M. Sajjadi, H. Komber, H. A. Khonakdar, and S. M. Sajadi, "In situ green synthesis of Cu-Ni bimetallic nanoparticles supported on reduced graphene oxide as an effective and recyclable catalyst for the synthesis of N-benzyl-N-aryl-5-amino-1H-tetrazoles," *Applied Organometallic Chemistry*, vol. 33, no. 7, p. e4938, 2019.

[16] A. Mujtaba and N. K. Janjua, "Fabrication and electrocatalytic application of CuO and Al_2O_3 hybrids," *Journal of the Electrochemical Society*, vol. 162, no. 6, pp. 328–337, 2015.

[17] L. Xiaodan, G. Min, M. Zhang, W. Xidong, G. Xiao, and C. Kuochih, "Effects of PVP on the preparation and growth mechanism of monodispersed Ni nanoparticles," *Rare Metals*, vol. 27, pp. 642–647, 2008.

[18] Z. Wei, P. Yan, W. Feng, J. Dai, Q. Wang, and T. Xia, "Microstructural characterization of Ni nanoparticles prepared by anodic arc plasma," *Materials Characterization*, vol. 57, pp. 176–181, 2006.

[19] B. Matheswaran, "Synthesis of iron oxide nanoparticles by using *Eucalyptus globulus* plant extract," *Journal of Surface Science and Nanotechnology*, vol. 12, pp. 363–367, 2014.

[20] L. Wilson, S. Zaccheus, J. Abigail, M. Buhari, and A. Musa, "Green synthesis, characterization and larvicidal activity of Cu/Ni bimetallic nanoparticles using fruit extract of palmyra palm," *International Journal of Cast Metals Research*, vol. 8, no. 1, pp. 20–25, 2020.

[21] H. F. Al-Rubai, A. K. Al-Dahan, and B. A. Jasim, "Green synthesis of iron oxide nanoparticles and their modification with CTAB for the decolorization of dye Reactive Blue 238," *Iraqi Journal of Science*, vol. 64, no. 4, pp. 1592–1600, 2023.

[22] M. A. Atiya, A. K. Hassan, and I. M. Luaibi, "Green synthesis of bimetallic iron/copper nanoparticles using *Ficus* leaves extract for removing Orange G (OG) dye from aqueous medium," *Nature Environment and Pollution Technology*, vol. 21, no. 1, pp. 355–365, 2022.

[23] J. Zhang and M. Qiu, "Adsorption kinetics and isotherms of copper ion in aqueous solution by bentonite supported nanoscale zero-valent iron," *Nature Environment and Pollution Technology*, vol. 18, no. 1, pp. 269–274, 2019.

[24] P. Sivakumar and P. N. Palanisamy, "Adsorption studies of basic red 29 by a non-conventional activated carbon prepared from *Euphorbia antiquorum* L," *International Journal of ChemTech Research*, vol. 1, no. 3, pp. 502–510, 2009.

[25] A. Sumaila, M. M. Ndamitso, Y. A. Iyaka, A. S. Abdulkareen, J. O. Tijani, and M. O. Idris, "Extraction and characterization of chitosan from crab shells: Kinetic and thermodynamic studies of arsenic and copper adsorption from electroplating wastewater," *Iraqi Journal of Science*, vol. 61, no. 9, pp. 2156–2171, 2020.

[26] U. D. Lingeswari and T. Vimala, "Isotherm, kinetic and thermodynamic study of adsorption of phthalocyanine and azo dyes by $CoCl_2$ doped polyaniline," *Asian Journal of Chemistry*, vol. 32, no. 4, pp. 746–752, 2020.

[27] R. T. Salim and D. E. Al-Mammar, "Adsorption of azo dye onto TiO_2 nanoparticles prepared by a novel green method: Isotherm and thermodynamic study," *Iraqi Journal of Science*, vol. 64, no. 8, pp. 3779–3792, 2023.